

Ground- γ band coupling in heavy deformed nuclei and SU(3) contraction limit

N. Minkov^{*1}, S. B. Drenska^{*2}, P. P. Raychev^{*3}, R. P. Roussev^{*4} and Dennis Bonatsos^{†5}

^{*} Institute for Nuclear Research and Nuclear Energy,
72 Tzarigrad Road, 1784 Sofia, Bulgaria

[†] Institute of Nuclear Physics, N.C.S.R. “Demokritos”,
GR-15310 Aghia Paraskevi, Attiki, Greece

Abstract

We derive analytic expressions for the energies and $B(E2)$ -transition probabilities in the states of the ground and γ bands of heavy deformed nuclei within a collective Vector-Boson Model with SU(3) dynamical symmetry. On this basis we examine the analytic behavior of the SU(3) energy splitting and the B(E2) interband transition ratios in the SU(3) contraction limits of the model. The theoretical analyses outline physically reasonable ways in which the ground- γ band coupling vanishes. The experimental data on the lowest collective states of even-even rare earth nuclei and actinides strongly support the theoretical results. They suggest that a transition from the ground- γ band coupling scheme to a scheme in which the ground band is situated in a separate irreducible representation of SU(3) should be realized towards the mid-shell regions. We propose that generally the SU(3) group contraction process should play an important role for such a kind of transitions in any collective band coupling scheme in heavy deformed nuclei.

PACS Numbers: 21.60.Fw, 21.60.Ev, 23.20.Js

¹e-mail: nminkov@inrne.bas.bg

²e-mail: sdren@inrne.bas.bg

³e-mail: raychev@bgcict.acad.bg

⁴e-mail: rousev@inrne.bas.bg

⁵e-mail: bonat@mail.demokritos.gr

1 Introduction

An important advantage of the dynamical symmetry (DS) approach [1, 2, 3, 4] in nuclear theory is the possibility to describe consistently various collective bands of heavy deformed nuclei [5, 6, 7]. Generally, the DS concept is based on the assumption that the physical system possesses a “primary” symmetry with respect to a given group, called DS group. The Hamiltonian of the system reduces this symmetry to the group of invariance of the system (which for the nuclear system coincides with the angular momentum group $SO(3)$) and thus the energy spectrum is generated [1]–[4]. The Lie algebra of the DS group is then reduced to the algebra of the group of invariance and is referred to as spectrum generating algebra. The basic idea of DS approach in heavy deformed nuclei is that their collective bands can be united into one or several multiplets, appearing in this reduction [5, 6, 7]. It provides a natural way to study the interaction between a particular couple of bands as well as the attendant spectroscopic characteristics of nuclei.

Various classification schemes with band coupling have been developed on the basis of DS approach. Well known models, such as the Interacting Boson Model (IBM) [8], the symplectic models [9, 10] and the Fermion Dynamical Symmetry Model [11], provide a good overall description of nuclear collective phenomena, covering the different regions of vibrational, rotational and transitional nuclei.

On the other hand, some models, based on the $SU(3)$ dynamical symmetry, reproduce successfully the particular characteristics of rotational bands in deformed nuclei. Such models are the Pseudo- $SU(3)$ Model [12], which has microscopic motivations, as well as the Vector-Boson Model (VBM) with $SU(3)$ dynamical symmetry [13, 14, 15], which allows a relevant phenomenological treatment of the $SU(3)$ multiplets in nuclei.

While in the $SU(3)$ limit of the IBM the possible irreducible representations (irreps) (λ, μ) are restricted by the total number of bosons describing the specific nucleus, in the VBM the possible $SU(3)$ irreps (λ, μ) are not restricted by the underlying theory. However, it has been shown recently [16] that some favored regions of (λ, μ) multiplets in the VBM could be outlined through the numerical analysis of the experimental data available for the ground (g) and the γ - collective bands of even–even deformed nuclei. (The favored multiplets provide the best model descriptions.) As a result, a systematic behavior of the $SU(3)$ symmetry properties of rotational nuclei has been established in terms of the VBM. It suggests the presence of a transition between a scheme, in which the g and the γ bands are coupled into one and the same (λ, μ) irrep and a scheme, where these two bands belong to different irreps. In addition it has been supposed that the fine systematic properties of rotational spectra could be interpreted as a manifestation of a more general dynamical symmetry.

As a first step in the recovering of the dynamical mechanism causing such a transition, one should study the way in which the $SU(3)$ symmetry is reduced in the (λ, μ) - plane. In particular, it is of interest to reproduce the limits, in which the quantum numbers λ and μ go to infinity, i.e. the cases, in which the $SU(3)$ irreps are not finite anymore. These limits correspond to the so called $SU(3)$ contraction process, in which the algebra of $SU(3)$ goes to the algebra of the semi-direct product $T_5 \wedge SO(3)$, i.e. $SU(3) \rightarrow T_5 \wedge SO(3)$ (T_5 is the group of 5-dimensional translations generated by the components of the $SU(3)$ -

quadrupole operators) [17, 18, 19, 20, 21, 22]. Generally, the contraction limit corresponds to a singular linear transformation of the basis of a given Lie algebra. The transformed structure constants approach a well-defined limits and a new Lie algebra, called contracted algebra, results [17]. The original and the contracted algebra are not isomorphic.

On the above basis it is expected that in the SU(3) contraction limit the space of the SU(3) irreps should undergo a respective limiting transition. As a result the SU(3) multiplets should be disintegrated to sets of various independent bands. It is, therefore, reasonable to consider this limit as a natural way in which the band-mixing interactions vanish. It is important to remark that the SU(3) contraction process is a situation in which a compact group goes to a non-compact one. Hence, one could try to interpret the vanishing g - γ band-mixing interaction as a transition from a compact to a non-compact DS group.

In the present work we realize the above considerations through the formalism of the VBM. Our purpose is to examine the various directions in the (λ, μ) -plane by investigating the respective changes in the structure of the SU(3) multiplets in terms of model defined spectroscopic characteristics of rotational nuclei. As such, we consider here the SU(3) energy splitting and the g - γ interband transitions, which carry important information about the link between the two bands. It is known that the energy splitting of the multiplet determines to a great extent the systematic behavior of the SU(3) dynamical symmetry in deformed nuclei [16].

In the VBM relatively simple analytic expressions for the energies and the transition probabilities can be derived both for the lowest $L = 2$ states of any (λ, μ) - multiplet and for all the states of any $(\lambda, 2)$ multiplet. The analytic expressions for the $L = 2$ states allow one to examine the SU(3) characteristics of nuclei in terms of two-dimensional surfaces in the (λ, μ) -plane, while in the $(\lambda, 2)$ direction one is able to investigate the behavior of the full set of states in the multiplet, i.e. the states with $L \geq 2$. On the other hand, the $L \geq 2$ states of the irreps with $\mu > 2$ can be treated numerically.

In such a way, a relevant combination of analytic and numerical analyses could be applied in order to reveal the systematic behavior of all the states of SU(3) irreps in the (λ, μ) -plane including the limiting cases of SU(3) group contraction. The collective scheme of the VBM is constructed by using the irreps with $\lambda \geq \mu$ and comprises the following two SU(3) contraction limits:

- (i) $\lambda \rightarrow \infty$, with μ finite;
- (ii) $\lambda \rightarrow \infty$, $\mu \rightarrow \infty$, with $\mu \leq \lambda$.

Below we provide a detailed study of the most important spectroscopic characteristics of the g and the γ band in the above limiting cases. It will be shown that our approach gives a reasonable interpretation of the corresponding experimental data and leads to rather clear conclusions about the rearrangement of collective rotational bands in heavy deformed nuclei.

In Sec. II the g - γ band coupling scheme of the VBM is briefly presented. In Sec. III we derive analytic expressions for the energies and the $B(E2)$ -transition probabilities for the 2_g and 2_γ states of an arbitrary (λ, μ) multiplet. Using them, we obtain the analytic behavior of the energy splitting and the physically meaningful transition ratios in the SU(3) contraction limits (i) and (ii). In Sec. IV we derive expressions for the splitting and the

transition ratios for the full set of states ($L \geq 2$) in the $(\lambda, 2)$ multiplets and obtain their analytic form in the first limiting case ($\lambda \rightarrow \infty$; $\mu = 2$). In Sec. V all analytic results are examined numerically. Also, there we provide a numerical study of the second limiting case ($\lambda \rightarrow \infty$, $\mu \rightarrow \infty$; $\mu \leq \lambda$) for the states with $L \geq 2$. The results are discussed together with an analysis of experimental data. In Sec. VI the conclusions are given.

2 g - γ band coupling in the VBM

The Vector-Boson Model (VBM) with SU(3) dynamical symmetry is founded on the assumption that the low-lying collective states of deformed even-even nuclei can be described by means of two distinct kinds of vector bosons, whose creation operators ξ^+ and η^+ are O(3) vectors and in addition transform according to two independent SU(3) irreps of the type $(\lambda, \mu) = (1, 0)$ [13, 14, 15]. The vector bosons provide a relevant construction of the SU(3) angular momentum and quadrupole operators like the bosons in the Schwinger realization of SU(2) [23]. Therefore, they can be considered as natural building blocks of a model scheme with SU(3) dynamical symmetry. Also, the vector bosons can be interpreted as quanta of elementary collective excitations of the nucleus [15].

In this model an SU(3)-symmetry reducing Hamiltonian is constructed by using three basic O(3) scalars, which belong to the enveloping algebra of SU(3) [13]:

$$V = g_1 L^2 + g_2 L \cdot Q \cdot L + g_3 A^+ A. \quad (1)$$

Here g_1 , g_2 and g_3 are free parameters; L and Q are the angular momentum and quadrupole operators respectively; and $A^+ = \xi^{+2} \eta^{+2} - (\xi^+ \cdot \eta^+)^2$.

The basis states

$$\left| \begin{array}{c} (\lambda, \mu) \\ \alpha, L, M \end{array} \right\rangle, \quad (2)$$

corresponding to the $SU(3) \supset O(3)$ group reduction, are constructed by means of the above vector-boson operators and are known as the basis of Bargmann-Moshinsky [24, 25].

The quantum number α in Eq. (2) distinguishes the various O(3) irreps, (L, M) , appearing in a given SU(3) irrep (λ, μ) and labels the different bands of an SU(3) multiplet. It is an integer number determined through the following inequality [14, 25]

$$\max\{0, \frac{1}{2}(\mu - L)\} \leq \alpha \leq \min\{\frac{1}{2}(\mu - \beta), \frac{1}{2}(\lambda + \mu - L - \beta)\}, \quad (3)$$

where

$$\beta = \begin{cases} 0, & \lambda + \mu - L \text{ even} \\ 1, & \lambda + \mu - L \text{ odd} \end{cases} \quad (4)$$

In the VBM the g - and the lowest γ - band belong to one and the same SU(3) multiplet, where λ and μ are even and $\lambda \geq \mu$. These bands are labeled by two neighboring integer values of the quantum number α . (More precisely, the states of the g - band are labeled by the largest value of α appearing in (3), while the γ - band corresponds to the next smaller α - value.) The so defined multiplet is split with respect to α .

The above scheme provides a good description of the energy levels and of the B(E2) transition ratios within and between the g - and γ - bands [13, 16]. The other collective bands, in particular the lowest β -band, do not belong to the same irrep. Therefore, they are not considered in the framework of this model.

3 The $L = 2$ states in (λ, μ) -plane

3.1 $L = 2$ energy splitting

Here we consider the $L = 2$ energy levels of the g - and the γ - band in terms of the VBM. For any (λ, μ) multiplet ($\mu \geq 2$), the 2_g and 2_γ states are the only possible ones appearing at angular momentum $L = 2$. They are labeled by the quantum number α as follows [See inequality (3)]: $\alpha_1 = \mu/2 - 1$ for 2_γ and $\alpha_2 = \mu/2$ for 2_g . Hence, for the $L = 2$ states the Hamiltonian matrix is always two-dimensional and the corresponding eigenvalue equation has the form:

$$\det \begin{pmatrix} V_{1,1} - \omega^{(2)} & V_{1,2} \\ V_{2,1} & V_{2,2} - \omega^{(2)} \end{pmatrix} = 0 , \quad (5)$$

where $\omega^{(2)} \equiv \omega^{L=2}$ are the eigenvalues and

$$V_{j,j'} \equiv \langle \alpha_j, 2 | V | \alpha_{j'}, 2 \rangle = \left\langle \begin{matrix} (\lambda, \mu) \\ \alpha_j, 2, 2 \end{matrix} \left| V \right| \begin{matrix} (\lambda, \mu) \\ \alpha_{j'}, 2, 2 \end{matrix} \right\rangle , \quad (6)$$

with $j, j' = 1, 2$, are the corresponding Hamiltonian matrix elements. We have derived these matrix elements in the form:

$$V_{1,1} = \langle (\frac{\mu}{2} - 1), 2 | V | (\frac{\mu}{2} - 1), 2 \rangle = 6g_1 + 6g_2(2\lambda + 2\mu + 3) + g_3P(\lambda, \mu) , \quad (7)$$

$$V_{2,2} = \langle \frac{\mu}{2}, 2 | V | \frac{\mu}{2}, 2 \rangle = 6g_1 - 6g_2(2\lambda + 2\mu + 3) + g_3Q(\lambda, \mu) , \quad (8)$$

$$V_{1,2} = \langle (\frac{\mu}{2} - 1), 2 | V | \frac{\mu}{2}, 2 \rangle = 12g_2\mu - 2g_3\mu(\mu - 2) , \quad (9)$$

$$V_{2,1} = \langle \frac{\mu}{2}, 2 | V | (\frac{\mu}{2} - 1), 2 \rangle = -12g_2\lambda + 2g_3\lambda(\lambda + 2\mu + 2) , \quad (10)$$

where

$$P(\lambda, \mu) = \lambda(\mu - 2)(\mu + 2)(\lambda + 2\mu + 2) + \mu(\mu - 2)(\mu + 1)(\mu + 3) , \quad (11)$$

$$Q(\lambda, \mu) = \lambda\mu^2(\lambda + 2\mu + 2) + \mu(\mu - 1)(\mu + 1)(\mu + 2) . \quad (12)$$

The energy levels E_2^g and E_2^γ , corresponding to the 2_g and 2_γ states respectively, are determined as

$$E_2^g = \omega_1^{(2)} - \omega^{(0)} , \quad (13)$$

$$E_2^\gamma = \omega_2^{(2)} - \omega^{(0)} , \quad (14)$$

where

$$\omega_i^{(2)} = \frac{1}{2} \left\{ V_{1,1} + V_{2,2} + (-1)^i \sqrt{(V_{1,1} + V_{2,2})^2 - 4(V_{1,1}V_{2,2} - V_{1,2}V_{2,1})} \right\} , \quad (15)$$

$i = 1, 2$, are the solutions of the eigenvalue equation (5), and $\omega^{(0)} = g_3\mu^2(\lambda + \mu + 1)^2$ is the zero-level eigenvalue, corresponding to the ground state 0_g . After using Eqs. (7)–(10) we obtain the following analytic expressions for E_2^g and E_2^γ :

$$E_2^g = 6g_1 - 2Fg_3 - 2\sqrt{Ag_2^2 + Bg_3^2 - Cg_2g_3} , \quad (16)$$

$$E_2^\gamma = 6g_1 - 2Fg_3 + 2\sqrt{Ag_2^2 + Bg_3^2 - Cg_2g_3} , \quad (17)$$

where

$$A = A(\lambda, \mu) = 9[(2\lambda + 2\mu + 3)^2 - 4\lambda\mu] ; \quad (18)$$

$$B = B(\lambda, \mu) = [\lambda(\lambda + 2\mu + 2) + \mu(\mu + 1)]^2 - \lambda\mu(\lambda + 2\mu + 2)(\mu - 2) ; \quad (19)$$

$$C = C(\lambda, \mu) = 6(2\lambda + 2\mu + 3)[\lambda(\lambda + 2\mu + 2) + \mu(\mu + 1)] - 6\lambda\mu(\lambda + 3\mu) ; \quad (20)$$

$$F = F(\lambda, \mu) = \lambda(\lambda + 2\mu + 2) + 2\mu(\mu + 1) . \quad (21)$$

Hence, we derive a model expression for the energy splitting of the SU(3) multiplet. It is known that the splitting can be characterized by the ratio [16]:

$$\Delta E_2 = \frac{E_2^\gamma - E_2^g}{E_2^g} . \quad (22)$$

In terms of Eqs. (16) and (17) the quantity ΔE_2 obtains the following analytic form:

$$\Delta E_2 = \frac{2}{(3g_1 - Fg_3)/\sqrt{Ag_2^2 + Bg_3^2 - Cg_2g_3} - 1} . \quad (23)$$

The expressions, obtained so far, allow us to study analytically the g – γ band-mixing interaction and the energy splitting at $L = 2$ in the (λ, μ) -plane. In particular we are able to reproduce analytically the SU(3) contraction limits:

(i) $\lambda \rightarrow \infty$, with μ finite;

(ii) $\lambda \rightarrow \infty$, $\mu \rightarrow \infty$, with $\mu \leq \lambda$. Since the difference $\lambda - \mu$ is always finite, we take for definiteness $\mu = \lambda$.

In each of these limits we estimate the λ - and/or μ - dependence of the matrix elements (7)–(10), as well as the analytic behavior of the splitting ratio ΔE_2 .

In case (i) the matrix elements are determined by the corresponding highest degrees of λ . Thus for $\mu > 2$ the Hamiltonian matrix $(V_{i,j})$ obtains the following asymptotic form:

$$(V)_{\lambda \rightarrow \infty} \sim \begin{pmatrix} \lambda^2 & * \\ \lambda^2 & \lambda^2 \end{pmatrix} , \quad (24)$$

where the upper off-diagonal element (denoted by $*$) does not depend on λ . Then the relative contribution of the off-diagonal (band-mixing) terms in the eigenvalue equation (5) decreases with the increase of λ as $\lambda^2/\lambda^4 = 1/\lambda^2$. For $\mu = 2$ the term $V_{1,1}$ is proportional

to λ instead of λ^2 [See Eqs. (7) and (11)], so that in this particular case the off-diagonal contribution decreases as $1/\lambda$.

In the same limiting case the functions (18)–(21) have the following asymptotic behavior:

$$A_{\lambda \rightarrow \infty} = 36\lambda^2; \quad B_{\lambda \rightarrow \infty} = \lambda^4; \quad C_{\lambda \rightarrow \infty} = 12\lambda^3; \quad F_{\lambda \rightarrow \infty} = \lambda^2 .$$

After applying them in Eq. (23), we find the analytic limit of the splitting ratio (23):

$$\lim_{\lambda \rightarrow \infty} \Delta E_2 = \frac{2}{-g_3/|g_3| - 1} . \quad (25)$$

We remark that the application of the VBM in rare earth nuclei and actinides requires $g_3 < 0$ [16], which gives in (25)

$$\lim_{\lambda \rightarrow \infty} \Delta E_2 = \infty . \quad (26)$$

Therefore, in this case the SU(3)-multiplet is completely split.

Consider now the limiting case (ii), $\lambda = \mu \rightarrow \infty$. Then the asymptotic form of the matrix ($V_{i,j}$) is:

$$(V)_{\lambda=\mu \rightarrow \infty} \sim \begin{pmatrix} \lambda^4 & \lambda^2 \\ \lambda^2 & \lambda^4 \end{pmatrix} . \quad (27)$$

Here we find that the relative magnitude of the band-mixing interaction decreases as $\lambda^4/\lambda^8 = 1/\lambda^4$, i.e., more rapidly in comparison to the previous case.

Furthermore, in the limiting case (ii) one has:

$$A_{\lambda=\mu \rightarrow \infty} = 108\lambda^2; \quad B_{\lambda=\mu \rightarrow \infty} = 13\lambda^4; \quad C_{\lambda=\mu \rightarrow \infty} = 72\lambda^3; \quad F_{\lambda=\mu \rightarrow \infty} = 5\lambda^2 .$$

Then the SU(3) splitting ratio goes to:

$$\lim_{\lambda=\mu \rightarrow \infty} \Delta E_2 = \frac{2}{-(5/\sqrt{13})g_3/|g_3| - 1} . \quad (28)$$

For $g_3 < 0$ we obtain

$$\lim_{\lambda=\mu \rightarrow \infty} \Delta E_2 = 2/(5/\sqrt{13} - 1) = 5.17 . \quad (29)$$

Therefore, in this case the band-mixing interaction vanishes, while the energy splitting between the two bands remains finite.

3.2 Transition ratios in the $L = 2$ states

Here we turn to the electromagnetic transition probabilities for the states 2_g , 2_γ and 0_g . In particular it is of interest to consider the following B(E2) transition ratios:

$$R_1(2) = \frac{B(E2; 2_\gamma \rightarrow 2_g)}{B(E2; 2_g \rightarrow 0_g)} ; \quad (30)$$

$$R_2(2) = \frac{B(E2; 2_\gamma \rightarrow 2_g)}{B(E2; 2_\gamma \rightarrow 0_g)} . \quad (31)$$

The first of them, $R_1(2)$, gives the relative magnitude of the g - γ interband transition probability with respect to the ground intraband one. Thus it naturally characterizes the link between the two bands within the multiplet. The second ratio represents one of the widely used collective characteristics of nuclei related to Alaga rules. Both quantities (30) and (31) can be obtained from the experimental data on deformed nuclei and therefore have a direct physical meaning.

In order to derive analytic expressions for the above ratios we calculate the matrix elements of the quadrupole operator Q_0 between the eigenstates

$$|\omega_i^{(2)}\rangle = C_{i1}^{(2)} \left| \begin{smallmatrix} (\lambda, \mu) \\ \mu/2 - 1, 2, 2 \end{smallmatrix} \right\rangle + C_{i2}^{(2)} \left| \begin{smallmatrix} (\lambda, \mu) \\ \mu/2, 2, 2 \end{smallmatrix} \right\rangle, \quad i = 1, 2; \quad (32)$$

$$|\omega^{(0)}\rangle = C^{(0)} \left| \begin{smallmatrix} (\lambda, \mu) \\ \mu/2, 0, 0 \end{smallmatrix} \right\rangle, \quad (33)$$

of the VBM Hamiltonian (1). (It should be remembered that the eigenvalues $\omega_1^{(2)}$, $\omega_2^{(2)}$ and $\omega^{(0)}$ correspond to the 2_g , 2_γ and 0_g states respectively.) After applying analytically the formalism developed in [16] we obtain the following matrix elements:

$$\langle \omega_1^{(2)} | Q_0 | \omega_2^{(2)} \rangle = \frac{4}{7} \frac{\lambda(C_{21}^{(2)})^2 + \mu(C_{22}^{(2)})^2 + (2\lambda + 2\mu + 3)C_{21}^{(2)}C_{22}^{(2)}}{C_{11}^{(2)}C_{22}^{(2)} - C_{21}^{(2)}C_{12}^{(2)}}; \quad (34)$$

$$\langle \omega_1^{(0)} | Q_0 | \omega_1^{(2)} \rangle = \sqrt{6}C^{(0)} \frac{\mu C_{22}^{(2)} - \lambda C_{21}^{(2)}}{C_{11}^{(2)}C_{22}^{(2)} - C_{12}^{(2)}C_{21}^{(2)}}; \quad (35)$$

$$\langle \omega^{(0)} | Q_0 | \omega_2^{(2)} \rangle = \sqrt{6}C^{(0)} \frac{\lambda C_{11}^{(2)} - \mu C_{12}^{(2)}}{C_{11}^{(2)}C_{22}^{(2)} - C_{12}^{(2)}C_{21}^{(2)}}. \quad (36)$$

The wave-function coefficients are determined as

$$C_{i1}^{(2)} = (f_{11}^{(2)} + 2h_{i2}f_{21}^{(2)} + h_{i2}^2f_{22}^{(2)})^{-\frac{1}{2}}; \quad (37)$$

$$C_{i2}^{(2)} = h_{i2}C_{i1}^{(2)}, \quad i = 1, 2 \quad (38)$$

$$C^{(0)} = (f^{(0)})^{-\frac{1}{2}}. \quad (39)$$

Here

$$f_{11}^{(2)} = \left\langle \begin{smallmatrix} (\lambda, \mu) \\ \mu/2 - 1, 2 \end{smallmatrix} \middle| \begin{smallmatrix} (\lambda, \mu) \\ \mu/2 - 1, 2 \end{smallmatrix} \right\rangle = \frac{1}{30} R(\lambda, \mu) \sum_{l=0}^{\mu-2} \left(\begin{smallmatrix} \mu/2 \\ l/2 \end{smallmatrix} \right) S^l(\lambda, \mu) \frac{(l+1)(\mu-l)}{\mu^2(\lambda+l+6)} \\ \times [(\mu-l)(\lambda+2)(\lambda+3)(\lambda+5) - \mu\lambda(\lambda+4)(\lambda+l+6)]; \quad (40)$$

$$f_{21}^{(2)} = \left\langle \begin{smallmatrix} (\lambda, \mu) \\ \mu/2, 2 \end{smallmatrix} \middle| \begin{smallmatrix} (\lambda, \mu) \\ \mu/2 - 1, 2 \end{smallmatrix} \right\rangle = \frac{1}{15} R(\lambda, \mu) \sum_{l=0}^{\mu-2} \left(\begin{smallmatrix} \mu/2 \\ l/2 \end{smallmatrix} \right) S^l(\lambda, \mu) \frac{(l+1)(\mu-l)}{\mu}; \quad (41)$$

$$f_{22}^{(2)} = \left\langle \begin{smallmatrix} (\lambda, \mu) \\ \mu/2, 2 \end{smallmatrix} \middle| \begin{smallmatrix} (\lambda, \mu) \\ \mu/2, 2 \end{smallmatrix} \right\rangle = \frac{1}{15} R(\lambda, \mu) \sum_{l=0}^{\mu} \left(\begin{smallmatrix} \mu/2 \\ l/2 \end{smallmatrix} \right) S^l(\lambda, \mu) (l+1)(l+2); \quad (42)$$

$$f^{(0)} = \left\langle \begin{pmatrix} \lambda, \mu \\ \mu/2, 0 \end{pmatrix} \middle| \begin{pmatrix} \lambda, \mu \\ \mu/2, 0 \end{pmatrix} \right\rangle = R(\lambda, \mu) \sum_{l=0}^{\mu} \binom{\mu/2}{l/2} S^l(\lambda, \mu) \frac{(\lambda + \mu - l)(\lambda + l + 4)}{\mu(\lambda + 3)(\lambda + \mu + 4)}, \quad (43)$$

are the corresponding overlap integrals obtained by the general expression in [14], with

$$R(\lambda, \mu) = (\lambda + 3)!!(\mu!!)^2, \quad (44)$$

$$S^l(\lambda, \mu) = ((l - 1)!!)^2 \frac{(\lambda + \mu - l - 2)!!(\lambda + \mu + 4)!!}{(\lambda + l + 4)!!}. \quad (45)$$

In addition [see Eqs. (13)–(15) in ref. [16]]

$$h_{i2} = -\frac{(V_{11} - \omega_i^{(2)})}{V_{12}} = \left[-3g_2(2\lambda + 2\mu + 3) + g_3[(\lambda + \mu)^2 + 2\lambda + \mu] + (-1)^i \sqrt{A(\lambda, \mu)g_2^2 + B(\lambda, \mu)g_3^2 - C(\lambda, \mu)g_2g_3} \right] / (6g_2\mu - g_3\mu(\mu - 2)), \quad (46)$$

with $A(\lambda, \mu)$, $B(\lambda, \mu)$ and $C(\lambda, \mu)$ being defined in Eqs. (18)–(20).

By using the general expression for the B(E2) transition probability between two of the above eigenstates

$$B(E2; L_\nu \rightarrow L'_{\nu''}) = \left(\begin{matrix} L' & 2 & L \\ -L & 0 & L \end{matrix} \right)^{-2} \left| \langle \omega_{\nu''}^{(L')} | Q_0 | \omega_\nu^{(L)} \rangle \right|^2 \quad (47)$$

($L, L' = 0, 2$; $\nu, \nu'' = g, \gamma$), we have studied analytically the transition ratios (30) and (31) in the two limiting cases considered in the previous subsection.

We have analyzed the explicit expressions for the overlap integrals (40)–(43) and the h_{i2} -factors (46). In this way we have deduced that in both limits, (i) and (ii), the overlap integrals increase to infinity. On the other hand one can verify that this behavior is compensated consistently in the ratios (30) and (31), where the total contribution of the integrals and the h_{i2} -factors is finite.

Thus, for the case (i) ($\lambda \rightarrow \infty$, with μ finite) we have obtained the following analytic limits of the transition ratios $R_1(2)$ and $R_2(2)$:

$$\lim_{\lambda \rightarrow \infty} \frac{B(E2; 2_\gamma \rightarrow 2_g)}{B(E2; 2_g \rightarrow 0_g)} = 0; \quad (48)$$

$$\lim_{\lambda \rightarrow \infty} \frac{B(E2; 2_\gamma \rightarrow 2_g)}{B(E2; 2_\gamma \rightarrow 0_g)} = \frac{10}{7} \left(\frac{\mu + 2}{2\mu} \right)^2. \quad (49)$$

So, in this case we find that the relative magnitude of the g – γ interband transition is zero, while the ratio $R_2(2)$ obtains finite values depending on the quantum number μ . We remark that for $\mu = 2$ one has $R_2(2) = 10/7$, which is the standard Alaga value.

In case (ii) ($\mu = \lambda \rightarrow \infty$) we obtain the following limits:

$$\lim_{\lambda=\mu \rightarrow \infty} \frac{B(E2; 2_\gamma \rightarrow 2_g)}{B(E2; 2_g \rightarrow 0_g)} = \frac{10}{7} \frac{(c_2^2 + 4c_2 + 1)^2}{(c_2^2 + c_2 + 1)(c_2 - 1)^2} \approx 0.172; \quad (50)$$

$$\lim_{\lambda=\mu \rightarrow \infty} \frac{B(E2; 2_\gamma \rightarrow 2_g)}{B(E2; 2_\gamma \rightarrow 0_g)} = \frac{10}{7} \frac{(c_2^2 + 4c_2 + 1)^2(c_1^2 + c_1 + 1)}{(c_2^2 + c_2 + 1)^2(c_1 - 1)^2} \approx 0.304, \quad (51)$$

with $c_1 = -4 - \sqrt{13} \approx -7.606$ and $c_2 = -4 + \sqrt{13} \approx -0.394$.

In this case one finds that both ratios, $R_1(2)$ and $R_2(2)$, remain finite.

We remark that all obtained limits do not depend on the model parameters. (It is assumed that g_1 , g_2 , and g_3 are finite, with $g_2 < 0$ and $g_3 < 0$.)

4 The $(\lambda, 2)$ -direction

4.1 $SU(3)$ splitting in $L \geq 2$ states

For the $(\lambda, 2)$ - irreps the g - and the γ -bands are the only possible ones appearing in the corresponding $SU(3)$ multiplets. They are labeled by the quantum numbers $\alpha_2 = 1$ and $\alpha_1 = 0$ respectively [See inequality (3)]. In the even angular momentum states the Hamiltonian matrix is always two-dimensional, while for the odd states of the γ - band one has a single matrix element. Hence for the $(\lambda, 2)$ - multiplets one is able to derive analytic expressions for the spectroscopic characteristics of the *full set of states* ($L \geq 2$) in a way similar to that of the previous section. That is why we do not explain in detail all steps of analytic calculations and report only the final results in this direction.

So, for a given $(\lambda, 2)$ multiplet the energy levels $E^g(L)$ and $E^\gamma(L)$ of the g and the γ -band can be written in the following form:

$$E^g(L) = \tilde{B} + \tilde{A}L(L+1) - |\tilde{B}|R^{(L)} , \quad (52)$$

$$E^\gamma(L_{\text{even}}) = \tilde{B} + \tilde{A}L(L+1) + |\tilde{B}|R^{(L)} ; \quad (53)$$

$$E^\gamma(L_{\text{odd}}) = 2\tilde{B} + (\tilde{A} + g_3)L(L+1) , \quad (54)$$

where

$$\tilde{A} = \tilde{A}(g_1, g_2, g_3) = g_1 - (2\lambda + 5)g_2 - g_3, \quad (55)$$

$$\tilde{B} = \tilde{B}(\lambda, g_2, g_3) = 6(2\lambda + 5)g_2 - 2(\lambda + 3)^2 g_3, \quad (56)$$

and

$$R^{(L)} = \sqrt{1 + aL(L+1) + bL^2(L+1)^2} . \quad (57)$$

with

$$a = a(\lambda, g_2, g_3) = -\frac{4}{\tilde{B}^2} \{(\lambda + 3)[(\lambda + 3)g_3 - 6g_2]g_3 - 3(g_3 - 6g_2)g_2\} , \quad (58)$$

$$b = b(\lambda, g_2, g_3) = \frac{1}{\tilde{B}^2} (g_3 - 6g_2)^2 . \quad (59)$$

Now we introduce the following energy ratio

$$\Delta E_L = \frac{E_L^\gamma - E_L^g}{E_2^g} , \quad (60)$$

which is more general compared to Eq.(22) and characterizes the magnitude of the energy splitting in any even angular momentum state of a given $SU(3)$ multiplet.

By using Eqs.(52) and (53) we obtain ΔE_L in the following analytic form

$$\Delta E_L = \frac{2|\tilde{B}|R^{(L)}}{6\tilde{A} - |\tilde{B}|R^{(2)} + \tilde{B}} , \quad (61)$$

which in the SU(3) contraction limit goes to

$$\lim_{\substack{\lambda \rightarrow \infty \\ \mu=2}} \Delta E_L = \frac{2}{-g_3/|g_3| - 1} . \quad (62)$$

For $g_3 < 0$ one has

$$\lim_{\substack{\lambda \rightarrow \infty \\ \mu=2}} \Delta E_L = \infty . \quad (63)$$

Thus we find that for all even states of a given $(\lambda, 2)$ - multiplet the SU(3) splitting goes to infinity in the same way [see also Eqs.(25) and (26)].

4.2 Transition ratios in the $(\lambda, 2)$ -direction

For the $(\lambda, 2)$ -direction the B(E2) transitions between the states of a given multiplet can be examined through the following [more general compared to (30) and (31)] transition ratios:

$$R_1(L) = \frac{B(E2; L_\gamma \rightarrow L_g)}{B(E2; L_g \rightarrow (L-2)_g)} , \quad L = \text{even} , \quad (64)$$

$$R_2(L) = \frac{B(E2; L_\gamma \rightarrow L_g)}{B(E2; L_\gamma \rightarrow (L-2)_g)} , \quad L = \text{even} , \quad (65)$$

$$R_3(L) = \frac{B(E2; L_\gamma \rightarrow (L+1)_g)}{B(E2; L_\gamma \rightarrow (L-1)_g)} , \quad L = \text{odd} . \quad (66)$$

The first two ratios, $R_1(L)$ and $R_2(L)$, have the same physical meaning as the ratios (30) and (31) of the previous section. The third ratio, $R_3(L)$, involves the odd angular momentum states in the study. In such a way we investigate the transition characteristics of the full set of states in a given SU(3) multiplet.

In the case of a $(\lambda, 2)$ -multiplet the Hamiltonian eigenstates are constructed as

$$|\omega_i^{(L)}\rangle = C_{i1}^{(L)} \left| \begin{smallmatrix} (\lambda, 2) \\ 0, L \end{smallmatrix} \right\rangle + C_{i2}^{(L)} \left| \begin{smallmatrix} (\lambda, 2) \\ 1, L \end{smallmatrix} \right\rangle , \quad i = 1, 2, L = \text{even}; \quad (67)$$

$$|\omega_{\text{odd}}^{(L)}\rangle = C_{\text{odd}}^{(L)} \left| \begin{smallmatrix} (\lambda, 2) \\ 0, L \end{smallmatrix} \right\rangle , \quad L = \text{odd}. \quad (68)$$

The necessary transition matrix elements are derived in the form

$$\begin{aligned} \langle \omega_1^{(L)} | Q_0 | \omega_2^{(L)} \rangle &= \frac{12}{(L+1)(2L+3)} [(\lambda+2-L)(C_{21}^{(L)})^2 \\ &+ [2\lambda+5+L(L-1)]C_{21}^{(L)}C_{22}^{(L)} \\ &+ L(L-1)(C_{22}^{(L)})^2] / [C_{11}^{(L)}C_{22}^{(L)} - C_{21}^{(L)}C_{12}^{(L)}] ; \end{aligned} \quad (69)$$

$$\begin{aligned}
\langle \omega_1^{(L-2)} | Q_0 | \omega_1^{(L)} \rangle &= \frac{6}{\sqrt{L(2L-1)}} \left[(\lambda + 4 - L) C_{11}^{(L-2)} C_{22}^{(L)} \right. \\
&\quad - (\lambda + 2 - L) C_{12}^{(L-2)} C_{21}^{(L)} \\
&\quad \left. + 2 C_{12}^{(L-2)} C_{22}^{(L)} \right] / \left[C_{11}^{(L)} C_{22}^{(L)} - C_{21}^{(L)} C_{12}^{(L)} \right] ; \quad (70)
\end{aligned}$$

$$\begin{aligned}
\langle \omega_1^{(L-2)} | Q_0 | \omega_2^{(L)} \rangle &= \frac{-6}{\sqrt{L(2L-1)}} \left[(\lambda + 4 - L) C_{11}^{(L-2)} C_{12}^{(L)} \right. \\
&\quad - (\lambda + 2 - L) C_{12}^{(L-2)} C_{11}^{(L)} \\
&\quad \left. + 2 C_{12}^{(L-2)} C_{12}^{(L)} \right] / \left[C_{11}^{(L)} C_{22}^{(L)} - C_{21}^{(L)} C_{12}^{(L)} \right] ; \quad (71)
\end{aligned}$$

$$\begin{aligned}
\langle \omega_1^{(L+1)} | Q_0 | \omega_2^{(L)} \rangle &= -\frac{6}{(L+2)\sqrt{L+1}} C_{\text{odd}}^{(L)} \left[(2\lambda - L + 4) C_{22}^{(L+1)} \right. \\
&\quad \left. + (\lambda - L + 1) C_{21}^{(L+1)} \right] / \left[C_{11}^{(L+1)} C_{22}^{(L+1)} - C_{21}^{(L+1)} C_{12}^{(L+1)} \right] ; \quad (72)
\end{aligned}$$

$$\langle \omega_1^{(L-1)} | Q_0 | \omega_2^{(L)} \rangle = -\frac{12}{(L+1)\sqrt{L}} \frac{1}{C_{\text{odd}}^{(L)}} \left[(\lambda - L + 3) C_{11}^{(L-1)} - (L - 1) C_{12}^{(L-1)} \right] , \quad (73)$$

with the wave-function coefficients

$$C_{i1}^{(L)} = \left(f_{11}^{(L)} + 2h_{i2}^{(L)} f_{21}^{(L)} + (h_{i2}^{(L)})^2 f_{22}^{(L)} \right)^{-\frac{1}{2}} , \quad L = \text{even} ; \quad (74)$$

$$C_{i2}^{(L)} = h_{i2}^{(L)} C_{i1}^{(L)} , \quad L = \text{even} , i = 1, 2 \quad (75)$$

$$C_{\text{odd}}^{(L)} = (f_{\text{odd}}^{(L)})^{-\frac{1}{2}} , \quad L = \text{odd} . \quad (76)$$

The corresponding overlap integrals are obtained in the form

$$f_{11}^{(L)} = \left\langle \begin{pmatrix} \lambda, 2 \\ 0, L \end{pmatrix} \middle| \begin{pmatrix} \lambda, 2 \\ 0, L \end{pmatrix} \right\rangle = S^L(\lambda) \frac{[(L^2 + L + 1)\lambda + L^3 + 4L^2 + 2L + 2]}{L(L-1)} ; \quad (77)$$

$$f_{21}^{(L)} = \left\langle \begin{pmatrix} \lambda, 2 \\ 1, L \end{pmatrix} \middle| \begin{pmatrix} \lambda, 2 \\ 0, L \end{pmatrix} \right\rangle = S^L(\lambda)(\lambda + L + 4) ; \quad (78)$$

$$f_{22}^{(L)} = \left\langle \begin{pmatrix} \lambda, 2 \\ 1, L \end{pmatrix} \middle| \begin{pmatrix} \lambda, 2 \\ 1, L \end{pmatrix} \right\rangle = S^L(\lambda) \frac{[2(\lambda - L + 2)(\lambda + L + 4) + (L + 1)(L + 2)]}{(\lambda - L + 2)} ; \quad (79)$$

$$f_{\text{odd}}^{(L)} = \left\langle \begin{pmatrix} \lambda, 2 \\ 0, L \end{pmatrix} \middle| \begin{pmatrix} \lambda, 2 \\ 0, L \end{pmatrix} \right\rangle = S_{\text{odd}}^L(\lambda) \frac{(L + 1)(L + 2)(\lambda + 2)}{2L(L - 1)} , \quad (80)$$

with

$$\begin{aligned} S^L(\lambda) &= \frac{2L!(\lambda - L + 2)!!(\lambda + L + 1)!!}{(2L + 1)!!} \\ S_{\text{odd}}^L(\lambda) &= \frac{2L!(\lambda - L + 1)!!(\lambda + L + 2)!!}{(2L + 1)!!} . \end{aligned} \quad (81)$$

Also we have

$$\begin{aligned} h_{i2}^{(L)} &= \left[-6g_2[(2\lambda + 5) + L(L - 1)] + g_3[2(\lambda + 3)^2 - L(L + 1)] \right. \\ &\quad \left. + (-1)^i \tilde{B}R^{(L)} \right] / [12g_2L(L - 1)] . \end{aligned} \quad (82)$$

Eqs. (77)–(80) show that the overlap integrals increase to infinity with the increase of the quantum number λ . However, similarly to the previous section, one can verify that this behavior is compensated consistently in the ratios (64)–(66).

After using the above analytic form of the matrix elements (69)–(73) we have obtained the SU(3) contraction limits of the ratios $R_1(L)$, $R_2(L)$ and $R_3(L)$ [Eqs. (64)–(66)]:

$$\lim_{\substack{\lambda \rightarrow \infty \\ \mu=2}} \frac{B(E2; L_\gamma \rightarrow L_g)}{B(E2; L_\gamma \rightarrow (L - 2)_g)} = 0 ; \quad (83)$$

$$\lim_{\substack{\lambda \rightarrow \infty \\ \mu=2}} \frac{B(E2; L_\gamma \rightarrow L_g)}{B(E2; L_\gamma \rightarrow (L - 2)_g)} = 6 \frac{(L - 1)(2L + 1)}{(L + 1)(2L + 3)} ; \quad (84)$$

$$\lim_{\substack{\lambda \rightarrow \infty \\ \mu=2}} \frac{B(E2; L_\gamma \rightarrow (L + 1)_g)}{B(E2; L_\gamma \rightarrow (L - 1)_g)} = \frac{(L - 1)}{(L + 2)} . \quad (85)$$

Thus, we find that for all the states ($L \geq 2$) of the Hamiltonian the relative magnitude of the g – γ interband transitions goes to zero. Also, we see that the ratios $R_2(L)$ and $R_3(L)$ go to the corresponding standard Alaga rules.

5 Results and Discussions

The theoretical results given above allow one to examine the mechanism of the SU(3) symmetry reduction in the space of the (λ, μ) irreps as well as to identify its manifestation in reference to the experimental data on heavy deformed nuclei.

The analytic study of the Hamiltonian matrix elements shows [Eqs. (24) and (27)] how the increase in the quantum numbers λ and/or μ is connected with the corresponding decrease in the g – γ band-mixing interaction within the framework of the SU(3) symmetry. Generally this result illustrates the behavior of the energy-mixing in the (λ, μ) -plane. In both limits, (i) and (ii), the g – γ mixing decreases asymptotically to zero. Similar limiting behavior of the $L \geq 2$ matrix elements in $(\lambda, 2)$ -direction has been established in our previous work (See Sec. IV–C of Ref. [16]). Thus in all limiting cases the SU(3) symmetry disappears completely and the two bands do not belong to the same SU(3) multiplet anymore.

It is appropriate at this point to elucidate the meaning of the above consideration in terms of the SU(3) group contraction process [18]–[22]. This process corresponds to a renormalization of the quadrupole operator, $Q \leftarrow Q/\sqrt{\langle C_2 \rangle}$, with

$$\langle C_2 \rangle = (\lambda + 2\mu)(\lambda + 2\mu + 6) + 3\lambda(\lambda + 2) \quad (86)$$

being the eigenvalue of the second order Casimir operator of SU(3). The following commutation relations between the angular momentum and the renormalized quadrupole operators are then valid:

$$[L_m, L_n] = -\sqrt{2}C_{1m1n}^{1m+n}L_{m+n}, \quad (87)$$

$$[L_m, Q_n] = \sqrt{6}C_{1m2n}^{2m+n}Q_{m+n}, \quad (88)$$

$$[Q_m, Q_n] = 3\sqrt{10}C_{2m2n}^{1m+n}\frac{L_{m+n}}{\langle C_2 \rangle}. \quad (89)$$

They differ from the standard SU(3) commutation relations by the factor $\langle C_2 \rangle$ in the right-hand side of (89). Taking into account Eq. (86), one finds that in both limits (i) and (ii), considered in the present work, the commutator (89) vanishes and the commutation relations of the algebra of the triaxial rotor group $T_5 \wedge SO(3)$ hold. In such a way the vanishing g – γ band-mixing could be interpreted as a transition from a compact to a non-compact DS group.

Let us now analyze the behavior of the splitting and transition ratios of Secs. 3 and 4 in the (λ, μ) -plane. For this purpose we use the analytic expressions for numerical calculations. In the particular case of $L \geq 2$ states in $(\mu = \lambda \rightarrow \infty)$ direction, which is not accessible analytically, we apply numerically the algorithm developed in Ref. [16]. All calculations are carried out for the same set of fixed model parameters $g_1 = 1$, $g_2 = -0.2$, $g_3 = -0.25$. These values belong to the corresponding parameter regions obtained for a group of rare earth nuclei and actinides [See Table 2 in Ref. [16]]. In this respect they can be considered as an overall set of model parameters. Also, it should be emphasized that in the SU(3) contraction limiting cases the various sets of (finite) parameter values give the same asymptotic behavior of the model quantities.

In Fig. 1 the splitting ratio ΔE_2 [Eq. (23)] is plotted as a function of the quantum numbers λ and μ . In the limiting case (i) ($\lambda \rightarrow \infty$, with μ finite) the two-dimensional surface shows a rapid increase of ΔE_2 , while in case (ii) ($\mu = \lambda \rightarrow \infty$) the splitting ratio gradually saturates towards the constant value ~ 5.17 [See Eq. (29)]. In Fig. 2 the splitting ratio ΔE_L [Eq. (60)] is plotted as a function of the quantum number λ for $L = 2, 4 \dots 12$. In the case $\lambda \rightarrow \infty$, $\mu = 2$ the energy splitting goes to infinity with almost equal values for all angular momenta (Fig. 2(a)). In case (ii) ΔE_L trends to finite values which increase with L (Fig. 2(b)). So, in the first limiting case the complete reduction of the SU(3) symmetry leads to a large energy separation between the bands in the multiplet, while in the second case (for finite angular momenta) the bands remain close to each other, but their mutual disposition does not depend on the Hamiltonian parameters anymore, so that it should not be associated with any band coupling.

The experimental ΔE_2 ratios of several rare earth nuclei and actinides are given in Table 1. They vary within the limits $5 \leq \Delta E_2 \leq 20$, for the rare earths and $13 \leq \Delta E_2 \leq 25$,

for the actinides. The behavior of the splitting ratios is clear: The ΔE_2 ratio generally increases towards the middle of the rotational region. This is illustrated in Table 1 through the number of the nucleon pairs (or holes) in the valence shells, N . (The number N is a well established characteristic of nuclear collectivity used in the IBM [8].) A clearly pronounced increase of ΔE_2 with increasing N is observed for the isotopes of Sm, Gd, Er, Yb, and W. Similar behavior of the energy splitting is observed in the $L > 2$ states of these nuclei [26]. One concludes that the data show that the SU(3) splitting increases toward the midshell regions.

We turn now to the analysis of the interband transition ratios. In Fig. 3 the theoretical ratio $R_1(2)$, Eq. (30), is plotted as a two-dimensional function of the quantum numbers λ and μ . In the limiting case (i) ($\lambda \rightarrow \infty$, with μ finite) the R_1 surface shows a rapid decrease to zero. In case (ii) ($\mu = \lambda \rightarrow \infty$) $R_1(2)$ decreases gradually and saturates towards the constant value ~ 0.172 [See Eq. (50)]. In Fig. 4 the transition ratio $R_1(L)$ [Eq. (64)] is plotted as a function of the quantum number λ for $L = 2, 4 \dots 12$. In the case $\lambda \rightarrow \infty$, $\mu = 2$ it goes to zero with almost equal values for all angular momenta (Fig. 4(a)). In case (ii) $R_1(L)$ obtains finite values which decrease with L (Fig. 4(b)). Thus in the first limiting case the $g\text{--}\gamma$ interband transition link vanishes rapidly, while in the second case (for finite angular momenta) the relative magnitude of the interband transition probability remains non-zero. However, as in the energy splitting, the R_1 -ratios do not depend on the Hamiltonian parameters anymore. Therefore, they should not be treated in terms of the SU(3) symmetry anymore.

The experimental $R_1(2)$ -values for several rare earth nuclei and actinides are given in Table 1. Here one observes a rather spectacular decrease of $R_1(2)$ towards the midshell regions. The best examples (with the largest number of available data) occur in the cases of the Gd, Er and Yb isotopes. Note that the decrease in the experimental $g\text{--}\gamma$ transition probabilities is well consistent with the corresponding increase in the SU(3) splitting. In this way, the experimental data strongly support the VBM predictions in the SU(3) contraction limit.

The two-dimensional surface obtained for the theoretical $R_2(2)$ ratio, Eq. (31), is shown in Fig. 5. We see that $R_2(2)$ gradually decreases with λ and μ and trends towards the finite values, obtained in the limiting cases (i) and (ii) [See Eqs. (49) and (51)]. In Fig. 6 the transition ratio $R_2(L)$ [Eq. (65)] is plotted as a function of the quantum number λ for $L = 2, 4 \dots 12$. In the case $\lambda \rightarrow \infty$, $\mu = 2$ it gradually goes to the Alaga values for the corresponding angular momenta (Fig. 6(a), see also Eq. (84)). In case (ii) $R_2(L)$ trends to finite values which (in the numerically investigated λ - range) exhibit a complicated behavior as a function of L (Fig. 6(b)). In both limiting cases the lack of dependence on the Hamiltonian parameters indicates the complete reduction of the SU(3) symmetry. The experimental data on $R_2(2)$, given in Table 1, show a slightly expressed trend of decreasing towards the midshells, but one could not draw any definite conclusions about the systematic behavior of this quantity.

In Fig. 7 the transition ratio $R_3(L)$ [Eq. (66)] is plotted as a function of the quantum number λ for the odd angular momenta $L = 3, 5 \dots 11$. For $\lambda \rightarrow \infty$, $\mu = 2$ it goes to the corresponding Alaga values in a way similar to the $R_2(L)$ - ratio (Fig. 7(a), see also

Eq. (85)). In the second direction, (ii), $R_3(L)$ saturates to finite values (Fig. 7(b)). It is clear that towards the SU(3) contraction limit the B(E2) transition characteristics of the odd γ band states should be consistent with the even angular momentum ones.

In order to assess quantitatively the results presented so far, we provide a numerical analysis of the SU(3) multiplets in (λ, μ) - plane on the basis of the experimental energy and transition ratios given in Table 1. More precisely we determined the quantum numbers λ and μ together with the Hamiltonian parameters g_1 , g_2 and g_3 , by fitting them in the numerical procedure of Ref. [16] so as to reproduce the experimental g - and γ - band levels up to $L = 8$, for lanthanides and $L = 18$, for actinides together with the values of the experimental ratios ΔE_2 , $R_1(2)$ and $R_2(2)$. (Only for two nuclei, ^{160}Gd and ^{162}Dy , the $R_1(2)$ ratios have not been used in the fits due to the uncertainty of the experimental data.)

The “favored” values of the quantum numbers λ and μ obtained for the various isotopes are given in the fourth column of Table 1. Generally the quantum number λ vary in the range $14 \leq \lambda \leq 68$, while μ obtains the values $2 \leq \mu \leq 6$.

So, one finds that while μ is closed in narrow limits, the quantum number λ exhibits a well pronounced systematic behavior. The favored λ -values as well as the SU(3) splitting ratio ΔE_2 increase with the increase of the valence pair number N , i.e. towards the middle of the valence shells in rotational nuclei. For example, the small splitting observed in the nuclei ^{152}Sm ($\Delta E_2 = 7.9$), ^{154}Gd ($\Delta E_2 = 7.1$) and ^{162}Er ($\Delta E_2 = 7.8$) which are situated near the beginning of the respective group of rotational isotopes, is associated with the small λ - values, $\lambda = 14 - 16$ and the relatively large interband transition ratios $R_1(2) = 0.07 - 0.08$. On the other hand, for the middshell nuclei $^{172,174}\text{Yb}$ with large splitting values, $\Delta E_2 = 18 - 20$ and small $R_1(2) \sim 0.01$, we obtain large λ -values, $\lambda \sim 60 - 70$. Also, large λ values, $\lambda \sim 60$ have been obtained for the $^{234,238}\text{U}$ isotopes with $\Delta E_2 = 20 - 22$. Well pronounced systematic behavior of the quantum number λ is observed in the Er and Yb isotopes.

The above results are consistent with the numerical analyses carried out in [16]. It should be mentioned that the involvement of the interband transition ratio $R_1(2)$ in the present fits leads to an increase in the quantum number μ above the $\mu = 2$ values. Actually, some trend of small increase in μ (up to $\mu = 6$) with the increase of λ is indicated for various isotope groups (See, for example the Yb isotopes in Table 1). Nevertheless, in almost all nuclei under study the quantum number λ is essentially larger than μ , which is natural for the well deformed nuclei. Several exceptions are observed in the nuclei far from the midshell region, such as ^{158}Dy (with $(\lambda, \mu) = (16, 6)$) and ^{186}W (with $(\lambda, \mu) = (24, 10)$) where the interband transition ratios are very large $R_1(2) \sim 0.1 - 0.2$.

The above quantitative considerations show that the changes in the SU(3) characteristics of nuclei (especially the quantum number λ) towards the middle of given rotational region could be associated with the corresponding decrease in the g - γ band mixing interaction towards the SU(3) contraction limits. In terms of our study the strong g - γ splitting, observed near the middle of rotational regions, corresponds to the weak mutual perturbation of the bands. This is consistent with the respectively good rotational behavior of the g -band, which in this case could belong to a separate SU(3) multiplet. [See the experimental

energy ratios, $R_4 = E_4^g/E_2^g$, given in Table 1.]

We remark that present analyses are based mainly on data in the rare earth region. Actually Table 1 includes only nuclei for which the g - γ interband transition probabilities are measured. That is why only four actinides ($^{230,232}\text{Th}$, $^{234,238}\text{U}$) are considered. Nevertheless, they give an indication for similar behaviors of the splitting and the interband transition ratios as the ones in rare earth nuclei. On the other hand, the generally stronger energy splitting, observed in the actinide region (See also [26]), suggests a generally weaker g - γ coupling compared to the rare earth nuclei.

We are now able to discuss the physical significance of the considered SU(3) contraction limits as well as to depict the physically meaningful directions in the (λ, μ) - plane, which could be appropriate for studying the transition between the different band coupling schemes. The theoretical analyses and experimental data show that the limiting case (i) ($\lambda \rightarrow \infty$, with μ finite) has a rather clear physical interpretation. It is consistent with the observed continuous increase of the g - γ band splitting and the corresponding continuous decrease of the interband transition probabilities towards the midshell regions in rare earth nuclei. The limiting case (ii) ($\lambda = \mu \rightarrow \infty$) does not have any similar direct interpretation. It suggests finite values for the splitting and the interband transition probabilities, while the bands do not interact in the framework of SU(3) symmetry. In addition, it is well known that the case $\lambda = \mu$ does not correspond to deformed nuclei, for which the inequality $\mu < \lambda$ is satisfied. Nevertheless the study of this limit is useful from the following viewpoint: It implies that the strong suppression of the band interaction as well as the transition between the different band coupling schemes could be realized at reasonable (finite) SU(3) splitting. Based on the above considerations, we deduce that the possibly interesting physically meaningful directions in the (λ, μ) -plane should be associated with a consistent increase in the quantum numbers λ and μ . Thus, any particular direction of interest could be easily estimated by using its intermediate behavior between the two considered limiting cases.

Some discussion concerning the Interacting Boson Model (IBM) classification scheme [8] is appropriate at this point. In Ref. [16] it has been suggested that for deformed nuclei both the VBM scheme (with g - γ band coupling) and the IBM one (with β - γ band coupling) could be considered as complementary schemes. It has also been pointed out that the SU(3) scheme of the VBM is naturally applicable to nuclei with weak energy splitting, while strong splitting invokes the SU(3) scheme of the IBM, in which the g - band is situated in a separate irrep. Furthermore, the theoretical results and the experimental data given in the present work suggest that the VBM band coupling scheme is more appropriate near the ends of the rotational regions, while in the midshell regions the coupling scheme of the IBM is realized. In this respect the detailed comparison of both band-coupling mechanisms would be of interest. For example, the analytic expressions for the g - γ interband transition probabilities, obtained in the framework of the IBM in [49], would be useful. [See Eqs. (5) and (6) of [49].] They give a behavior of the transition ratios $R_1(L)$, $R_2(L)$ and $R_3(L)$ [Eqs. (64), (65) and (66)] in the infinite valence pair number limit ($N \rightarrow \infty$) similar to the behavior obtained in the limiting case (i) ($\lambda \rightarrow \infty$, with $\mu = 2$) [Eqs. (83), (84) (85)] of the present VBM scheme.

As an extension of the present studies it would be worthwhile to examine, in a similar way, the link between the γ - and the β - band. Furthermore, besides the VBM scheme, one could refer in this case to the modifications of the IBM in which higher-order terms conserving the SU(3) symmetry are added [50]. The consistent study (within both models) of the ways in which the SU(3) symmetry is reduced could give important information about the rearrangement of rotational bands into different SU(3) irreps.

In the above context, we emphasize that the analyses implemented in the presented paper give a general prescription to handle the fine behavior of the band coupling interactions in any collective algebraic scheme in heavy deformed nuclei. Actually, the group contraction process should play a major role in a transition between two different band coupling schemes. The transition from the compact SU(3) group to the non-compact $T_5 \wedge SO(3)$ rotor group could be considered as a starting point in a process of reconstruction of various multiplets in a more general symplectic group of dynamical symmetry. (It is interesting to mention that the meaning of SU(3) contraction has been also discussed (though in a rather different aspect) in reference to a possible phase transition between a superconductor and rigid rotor collective motion of nuclei [51].)

6 Conclusions

We have derived analytic expressions for the energies and $B(E2)$ transition probabilities in the ground- and γ -band states of even deformed nuclei within the Vector-Boson Model with SU(3) dynamical symmetry. On this basis we applied both analytic and numeric analyses to examine the behavior of the corresponding energy splitting and $B(E2)$ transition ratios in the two SU(3) contraction limits of the model, (i) ($\lambda \rightarrow \infty$, with μ finite), and (ii) ($\lambda = \mu \rightarrow \infty$). It has been shown that in both limits the g - γ band mixing decreases asymptotically to zero. In case (i) this is associated with the corresponding continuous increase in the splitting of the multiplet and the rapidly vanishing g - γ interband transition link. Case (ii) gives finite values for the energy splitting and the interband transition ratios which, however, should not be associated with any band coupling. The latter result implies that a strong reduction of the band interaction could be possible at finite SU(3) splitting. Thus, the present analyses outline the possible directions in the (λ, μ) -plane in which the g - γ band coupling is reduced.

The experimental data on the ground- and γ - band states in deformed even-even nuclei show clearly a pronounced increase in the g - γ band splitting and a corresponding decrease in the interband transition probabilities towards the midshell regions. They suggest that the SU(3) contraction effects in the g - γ band coupling scheme should be sought in the best rotational nuclei, in which the mutual perturbation of the bands is weak. So, the experimental data and their quantitative estimation in the VBM framework strongly support our theoretical analyses.

Based on the presented investigation, we conclude that the transition from the g - γ band coupling scheme to a scheme in which the g -band is situated in a separate irrep should be realized towards the midshell regions. In this respect the complementarity of the classification schemes of the Vector-Boson Model with SU(3) dynamical symmetry and

the IBM becomes clear. The consistent study of the rearrangement of collective bands in deformed nuclei, including the β - excited bands, will be the subject of forthcoming work.

Acknowledgments

The authors are thankful to P. Van Isacker for stimulating discussions and D. N. Kadrev for the help in collecting the experimental data. This work has been supported by the Bulgarian National Fund for Scientific Research under contract no MU-F-02/98.

References

- [1] A. O. Barut, Phys. Rev. B **135**, 839 (1964).
- [2] Y. Dothan, M. Gell-Mann and Y. Neeman, Phys. Lett. **17**, 148 (1965).
- [3] N. Mukunda, L. O' Raifeartaigh and E. Sudarshan, Phys. Rev. Lett. **15**, 1041 (1965); Phys. Lett. **19**, 322 (1965).
- [4] R. F. Dashen and M. Gell-Mann, Phys. Lett. **17**, 142 (1965).
- [5] L. Weaver and L. C. Biedenharn, Phys. Rev. Lett. **32B**, 326 (1970).
- [6] P. P. Raychev, Sov. J. Nucl. Phys. **16**, 643 (1972).
- [7] G. Afanasjev and P. Raychev, Part. and Nucl. **3**, 436 (1972).
- [8] F. Iachello and A. Arima, *The Interacting Boson Model* (Cambridge University Press, Cambridge, 1987).
- [9] G. Rosensteel and D. J. Rowe, Ann. Phys. (N.Y.) **96**, 1 (1976).
- [10] G. F. Filippov, V. I. Ovcharenko and Yu. F. Smirnov, *Microscopic Theory of Nuclear Collective Excitations* (Naukova Dumka, Kiev, 1981).
- [11] C. L. Wu, D. H. Feng, X. G. Chen, J. Q. Chen and M. W. Guidry, Phys. Lett. B **168**, 313 (1986).
- [12] J. P. Draayer and K. J. Weeks, Ann. Phys. (N.Y.) **156**, 41 (1984).
- [13] P. P. Raychev and R. P. Roussev, Sov. J. Nucl. Phys. **27**, 1501 (1978).
- [14] S. Alisauskas, P. P. Raychev and R. P. Roussev, J. Phys. G **7**, 1213 (1981).
- [15] P. P. Raychev and R. P. Roussev, J. Phys. G **7**, 1227 (1981).
- [16] N. Minkov, S. Drenska, P. Raychev, R. Roussev and D. Bonatsos, Phys. Rev. C **55**, 2345 (1997).
- [17] R. Gilmore, *Lie Groups, Lie Algebras and Some of Their Applications* (Wiley, New York, 1974).
- [18] J. Carvalho, R. Le Blanc, M. Vassanji and D. J. Rowe, Nucl. Phys. **A452**, 240 (1986).
- [19] O. Castaños, J. P. Draayer and Y. Leschber, Z. Phys. A **329**, 33 (1988).
- [20] D. J. Rowe, M. G. Vassanji and J. Carvalho, Nucl. Phys. **A504**, 76 (1989).
- [21] M. Mukerjee, Phys. Lett. **251B**, 229 (1990).

- [22] J. P. Draayer, in *Algebraic Approaches to Nuclear Structure: Interacting Boson and Fermion Models*, Contemporary Concepts in Physics VI, edited by R. F. Casten (Harwood, Chur, 1993) p. 423.
- [23] L. C. Biedenharn and J. D. Louck, *Angular Momentum in Quantum Physics*, Encyclopedia of Mathematics and its Applications **8** (Addison Wesley, Reading, 1981).
- [24] V. Bargmann and M. Moshinsky, Nucl. Phys. **23**, 177 (1961).
- [25] M. Moshinsky, J. Patera, R. T. Sharp and P. Winternitz, Ann. Phys. (N.Y.) **95**, 139 (1975).
- [26] M. Sakai, At. Data Nucl. Data Tables **31**, 399 (1984).
- [27] A. Artna-Cohen, NDS **79**, 1 (1996).
- [28] R. G. Helmer, NDS **69**, 507 (1993).
- [29] W. Andrejtscheff and P. Petkov, private communication.
- [30] R. G. Helmer, NDS **65**, 65 (1992).
- [31] M. A. Lee, NDS **56**, 199 (1989).
- [32] M. A. Lee and R. L. Bunting, NDS **46**, 187 (1985).
- [33] S. Raman, C. H. Malarkey, W. T. Milner, C. W. Nestor Jr., and P. H. Stelson, At. Data Nucl. Data Tables **36**, 1 (1987).
- [34] R. G. Helmer, NDS **64**, 79 (1991).
- [35] E. N. Shurshikov, NDS **47**, 433 (1986).
- [36] E. N. Shurshikov and N. V. Timofeeva, NDS **67**, 45 (1992).
- [37] V. S. Shirley, NDS **53**, 223 (1988).
- [38] C. M. Baglin, NDS **77**, 125 (1996).
- [39] G. Q. Wang, NDS **51**, 577 (1987).
- [40] E. Browne, NDS **62**, 1 (1991).
- [41] E. Browne, NDS **60**, 227 (1990).
- [42] E. Browne, NDS **54**, 199 (1988).
- [43] R. B. Firestone, NDS **58**, 243 (1989).
- [44] R. B. Firestone, NDS **55**, 583 (1988).

- [45] Y. A. Ellis-Akovali, NDS **40**, 385 (1983).
- [46] M. R. Schmorak, NDS **36**, 367 (1982).
- [47] Y. A. Ellis-Akovali, NDS **40**, 523 (1983).
- [48] E. N. Shurshikov, NDS **53**, 601 (1988).
- [49] P. Van Isacker, Phys. Rev. C **27**, 2447 (1983).
- [50] G. Van den Berghe, H. E. De Meyer and P. Van Isacker, Phys. Rev. C **32**, 1049 (1985).
- [51] C. Bahri, D. J. Rowe and W. Wijesundera, Phys. Rev. C **58**, 1539 (1998).

Table 1: Experimental values of the energy splitting (Eq. (22), column 5) and B(E2)-interband transition ratios in the 2_g and 2_γ states (Eq. (30) in column 6, Eq. (31) in column 7) of deformed rare earth nuclei and actinides. The corresponding favored SU(3)-quantum numbers (λ, μ) are given in column 4. The valence pair number, N , as well as the $R_4 = E_4^g/E_2^g$ energy ratio are also given in columns 2 and 3 respectively. Data are taken from [26], for the energies and from the Refs. in the last column, for the transition probabilities.

Nucl.	N	$R_4 = \frac{E_4^g}{E_2^g}$	(λ, μ)	$\Delta E_2 = \frac{E_2^\gamma - E_2^g}{E_2^g}$	$R_1(2) = \frac{2_\gamma \rightarrow 2_g}{2_g \rightarrow 0_g}$	$R_2(2) = \frac{2_\gamma \rightarrow 2_g}{2_\gamma \rightarrow 0_g}$	Ref.
^{152}Sm	10	3.009	(14,4)	7.915	0.065 (5)	2.56 (26)	[27]
^{154}Sm	11	3.253	(58,6)	16.565	0.022	1.35	[28], [29]
^{154}Gd	11	3.015	(14,4)	7.093	0.083 (6)	2.15 (24)	[28]
^{156}Gd	12	3.239	(24,4)	11.969	0.039 (3)	1.56 (12)	[30]
^{158}Gd	13	3.288	(28,4)	13.932	0.029 (4)	1.71 (41)	[31]
^{160}Gd	14	3.298	(22,2)	12.128	$\leq 10^{-3}$	1.69 (19)	[32], [33]
^{158}Dy	13	3.207	(16,6)	8.567	0.103 (23)	3.22 (133)	[31]
^{160}Dy	14	3.270	(16,2)	10.131	0.028 (9)	1.93 (112)	[32]
^{162}Dy	15	3.294	(16,2)	10.007	$\leq 10^{-3}$	1.66	[34]
^{164}Dy	16	3.301	(16,2)	9.379	0.038 (4)	2.00 (38)	[35]
^{162}Er	13	3.229	(16,4)	7.822	0.067 (11)	2.37 (35)	[34]
^{164}Er	14	3.277	(18,4)	8.412	0.052 (7)	2.19 (48)	[35]
^{166}Er	15	3.289	(20,4)	8.751	0.045 (5)	1.76 (26)	[36]
^{168}Er	16	3.309	(22,4)	9.291	0.0410 (3)	1.80 (12)	[37]
^{170}Er	17	3.310	(30,4)	10.858	0.034 (7)	1.93 (36)	[38]
^{168}Yb	14	3.266	(14,2)	10.218	0.046 (6)	2.09 (72)	[37]
^{170}Yb	15	3.293	(18,2)	12.594	0.024 (6)	1.78 (77)	[38]
^{172}Yb	16	3.305	(58,4)	17.602	0.011 (3)	1.45 (65)	[39], [29]
^{174}Yb	17	3.310	(68,6)	20.356	0.012 (3)	2.40 (94)	[40]
^{176}Yb	16	3.308	(42,4)	14.358	0.018 (4)	1.94 (70)	[41]
^{174}Hf	15	3.268	(36,6)	12.481	0.049 (12)	1.54 (63)	[40]
^{178}Hf	15	3.291	(30,4)	11.604	0.028 (2)	1.18 (19)	[42]
^{182}W	13	3.291	(18,4)	11.203	0.053 (6)	1.90 (19)	[29]
^{184}W	12	3.274	(16,4)	7.123	0.071 (5)	1.91 (19)	[43]
^{186}W	11	3.242	(24,10)	5.030	0.181 (13)	2.27 (32)	[44]
^{230}Th	11	3.272	(24,4)	13.586	0.028 (5)	1.83 (53)	[45]
^{232}Th	12	3.284	(26,4)	14.893	0.036 (6)	2.73 (62)	[46]
^{234}U	13	3.296	(58,6)	20.304	0.021 (5)	1.69 (69)	[47]
^{238}U	15	3.304	(60,6)	22.614	0.019 (1)	1.75 (17)	[48]

Figure Captions

Figure 1. The theoretical energy splitting ratio ΔE_2 [Eq. (23)] is plotted as a two-dimensional function of the quantum numbers λ and μ for $g_1 = 1$, $g_2 = -0.2$ and $g_3 = -0.25$.

Figure 2. The theoretical energy splitting ratio ΔE_L [Eq. (60)] is plotted as a function of the quantum number λ for $L = 2, 4 \dots 12$ with $g_1 = 1$, $g_2 = -0.2$ and $g_3 = -0.25$ in the cases: (a) $\mu = 2$; (b) $\mu = \lambda$.

Figure 3. The theoretical $R_1(2)$ ratio [Eq. (30)] is plotted as a two-dimensional function of the quantum numbers λ and μ for $g_2 = -0.2$ and $g_3 = -0.25$.

Figure 4. The theoretical $R_1(L)$ ratio [Eq. (64)] is plotted as a function of the quantum number λ for $L = 2, 4 \dots 12$ with $g_2 = -0.2$ and $g_3 = -0.25$ in the cases: (a) $\mu = 2$; (b) $\mu = \lambda$.

Figure 5. The same as Fig. 3 but for the theoretical $R_2(2)$ ratio [Eq. (31)].

Figure 6. The same as Fig. 4 but for the theoretical $R_2(L)$ ratio [Eq. (65)].

Figure 7. The theoretical $R_3(L)$ ratio [Eq. (66)] is plotted as a function of the quantum number λ for $L = 3, 5 \dots 11$ with $g_2 = -0.2$ and $g_3 = -0.25$ in the cases: (a) $\mu = 2$; (b) $\mu = \lambda$.

Figure 1

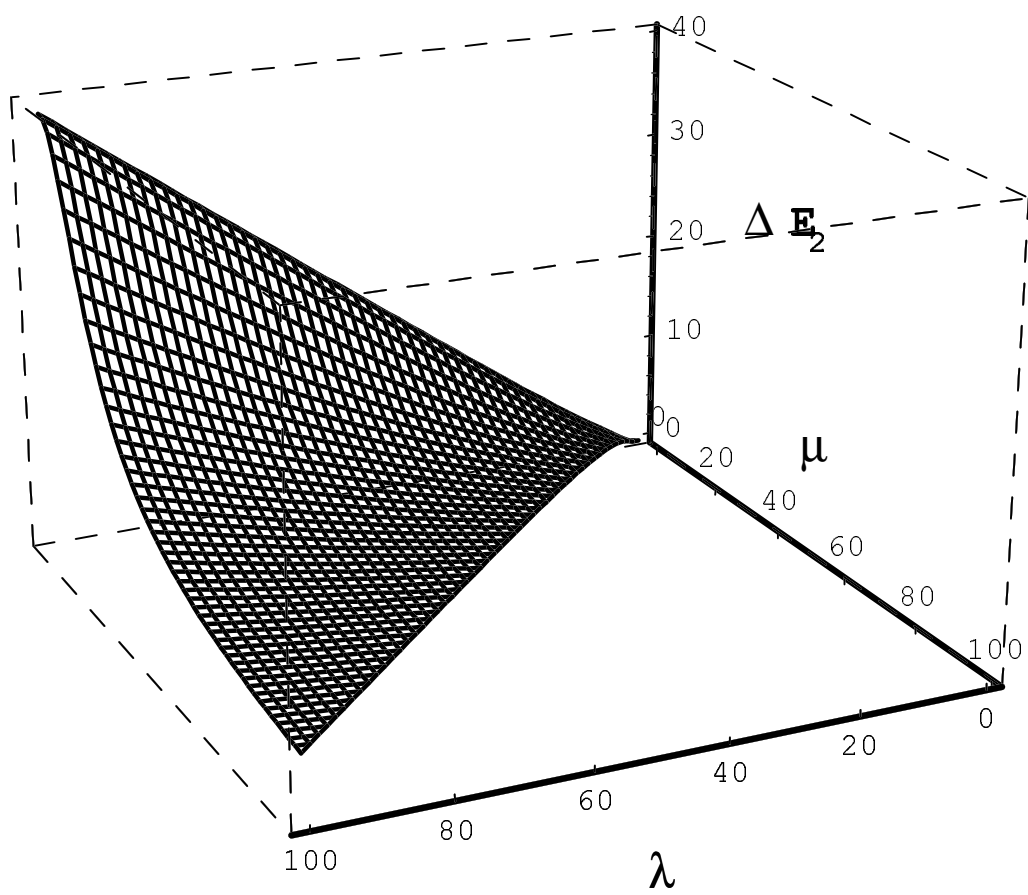


Figure 2(a)

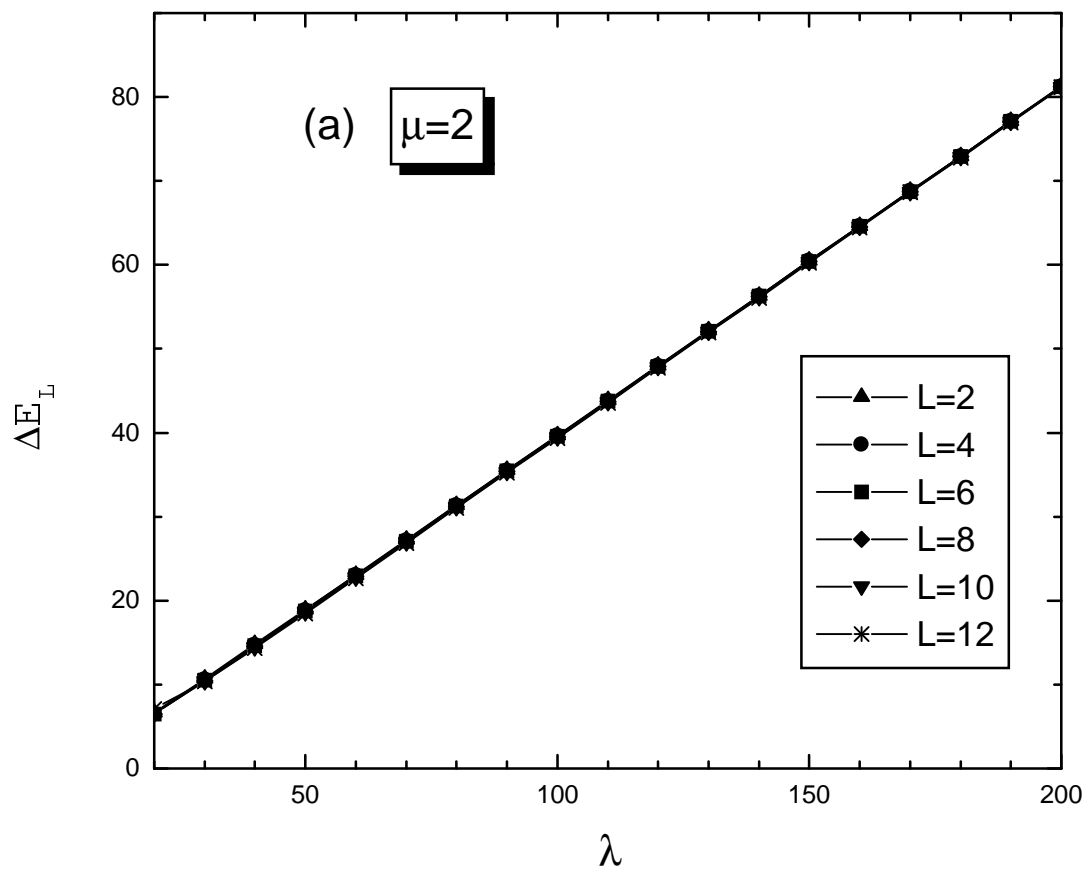


Figure 2(b)

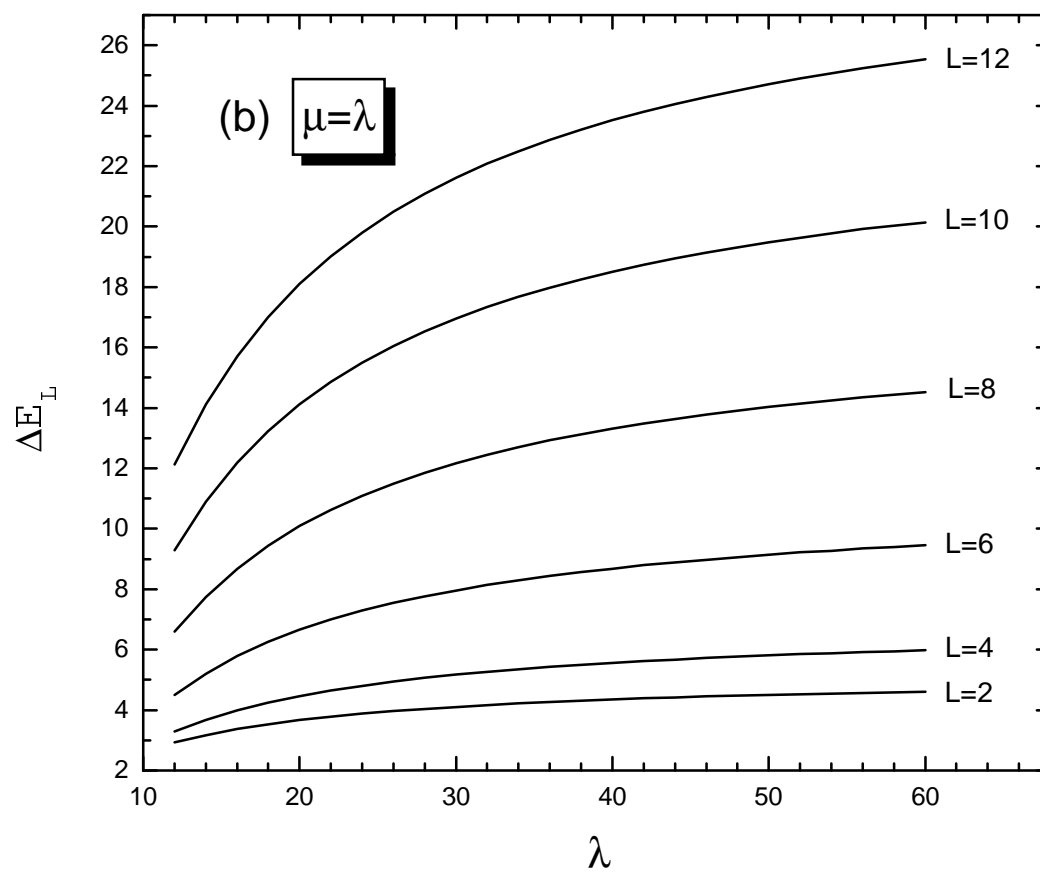


Figure 3

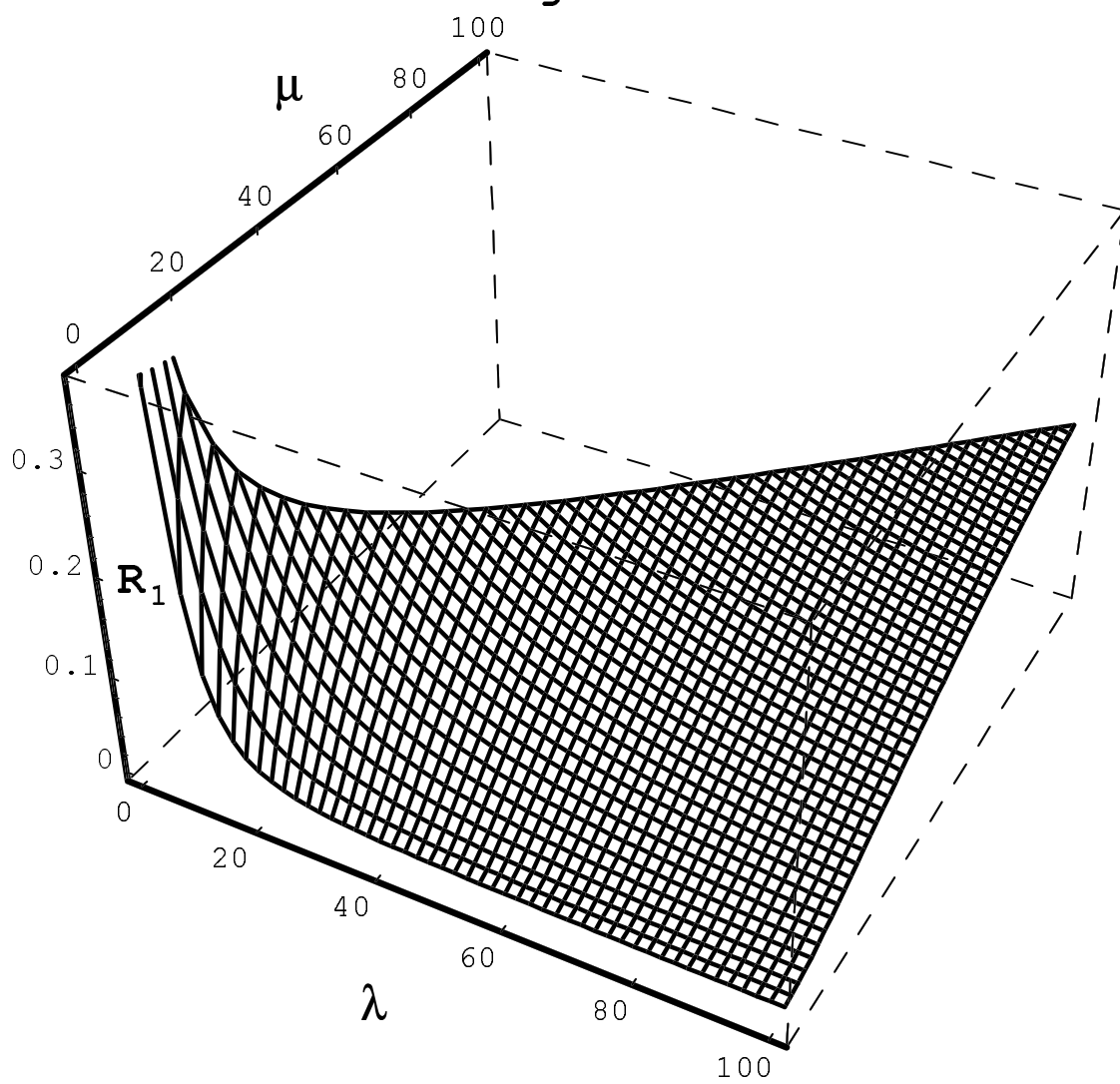


Figure 4(a)

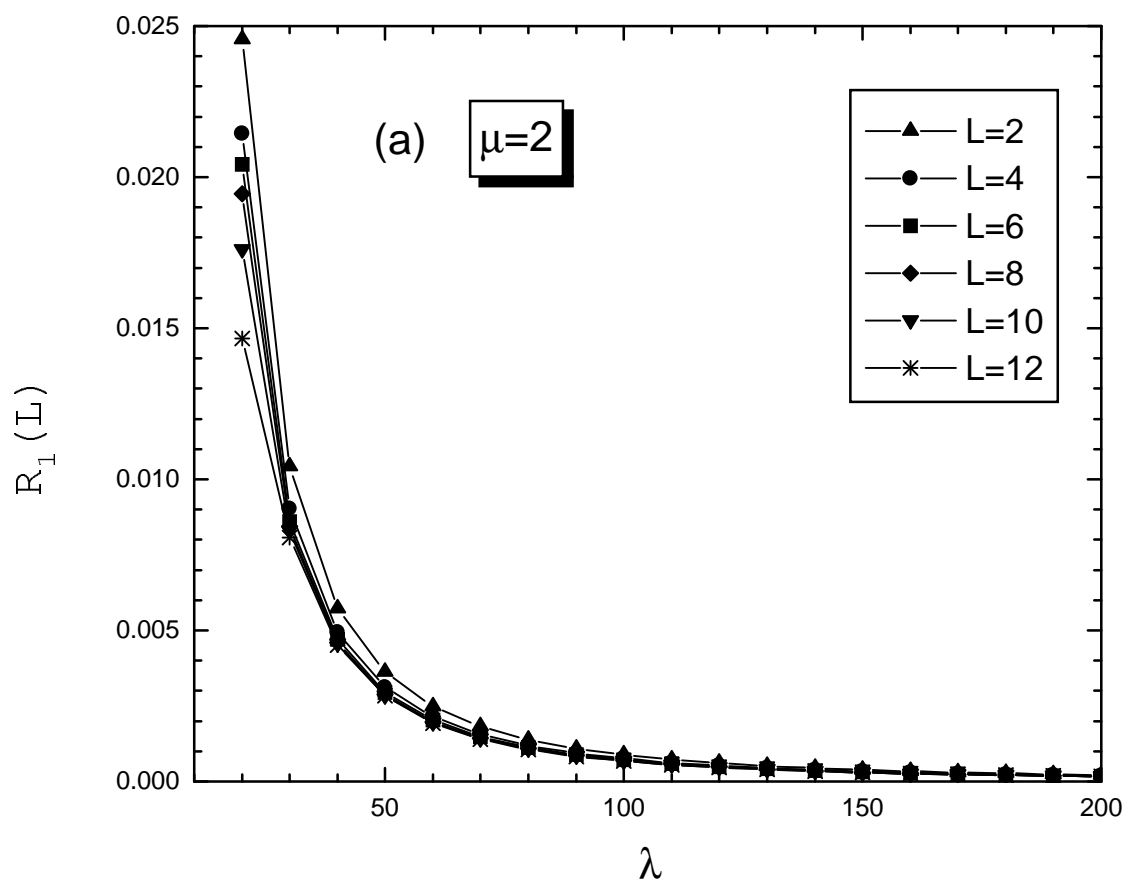


Figure 4(b)

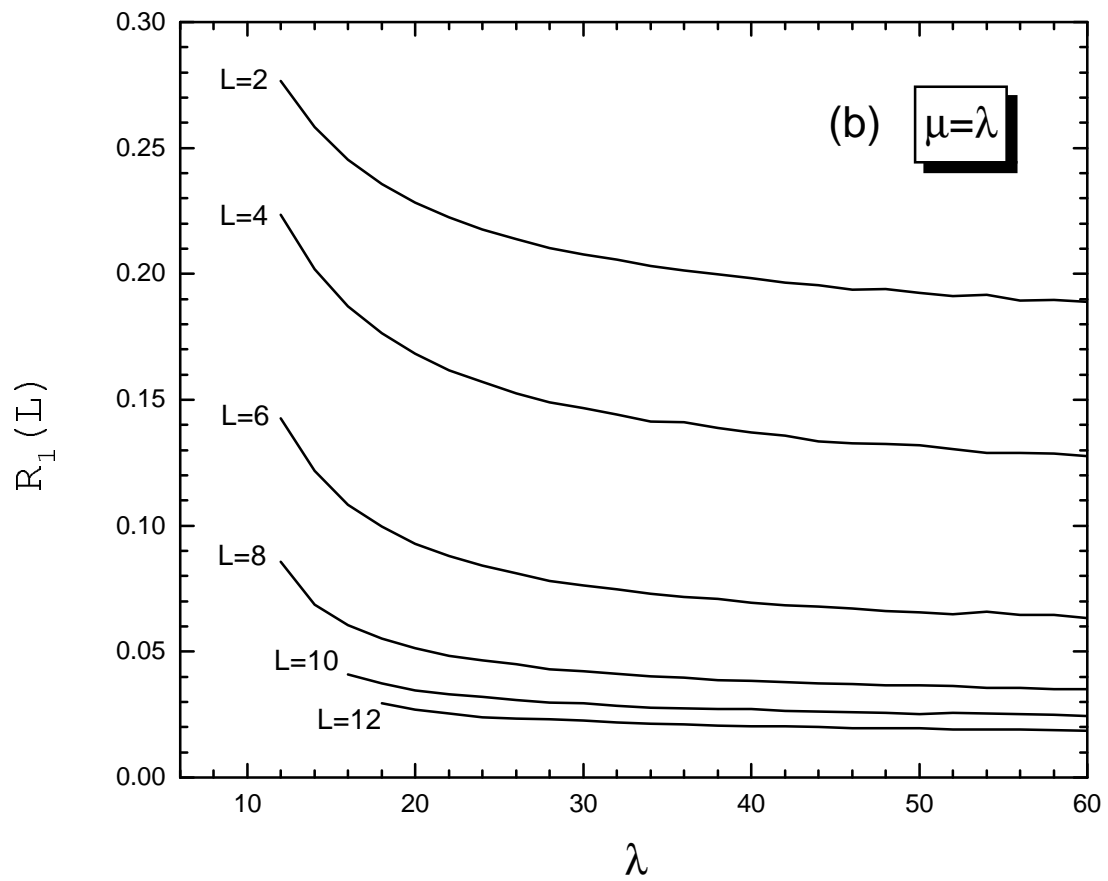


Figure 5

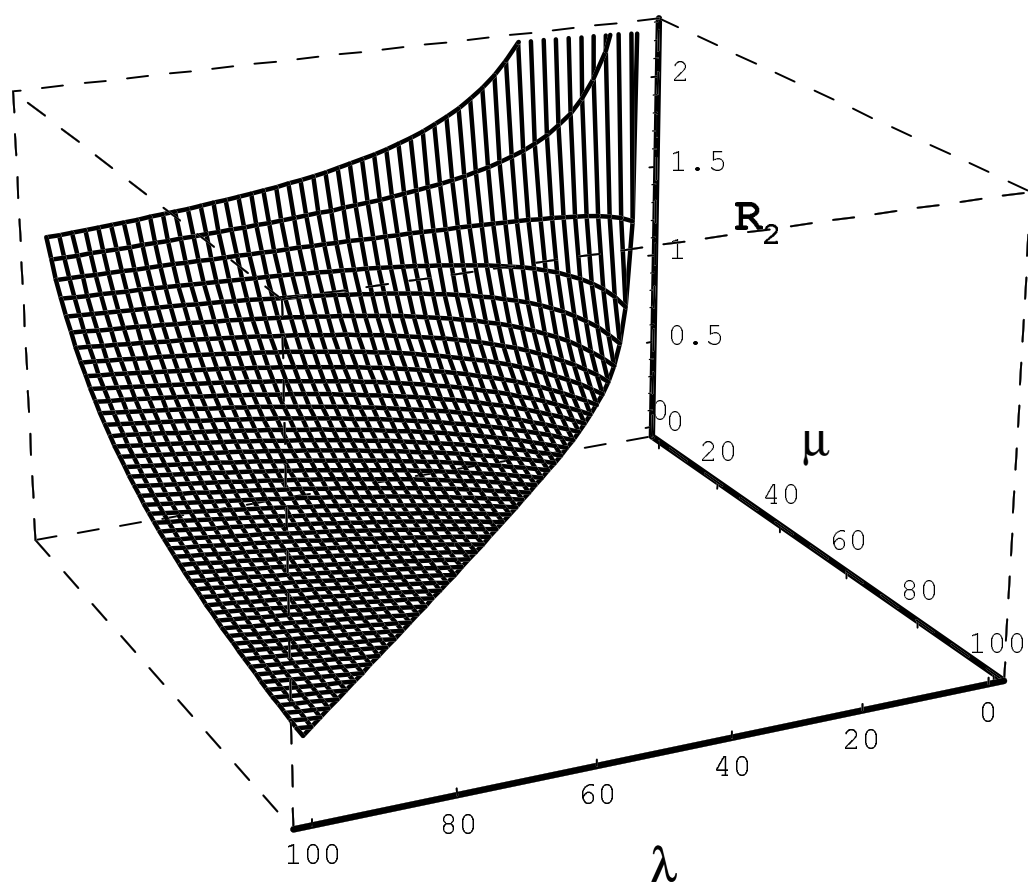


Figure 6(a)

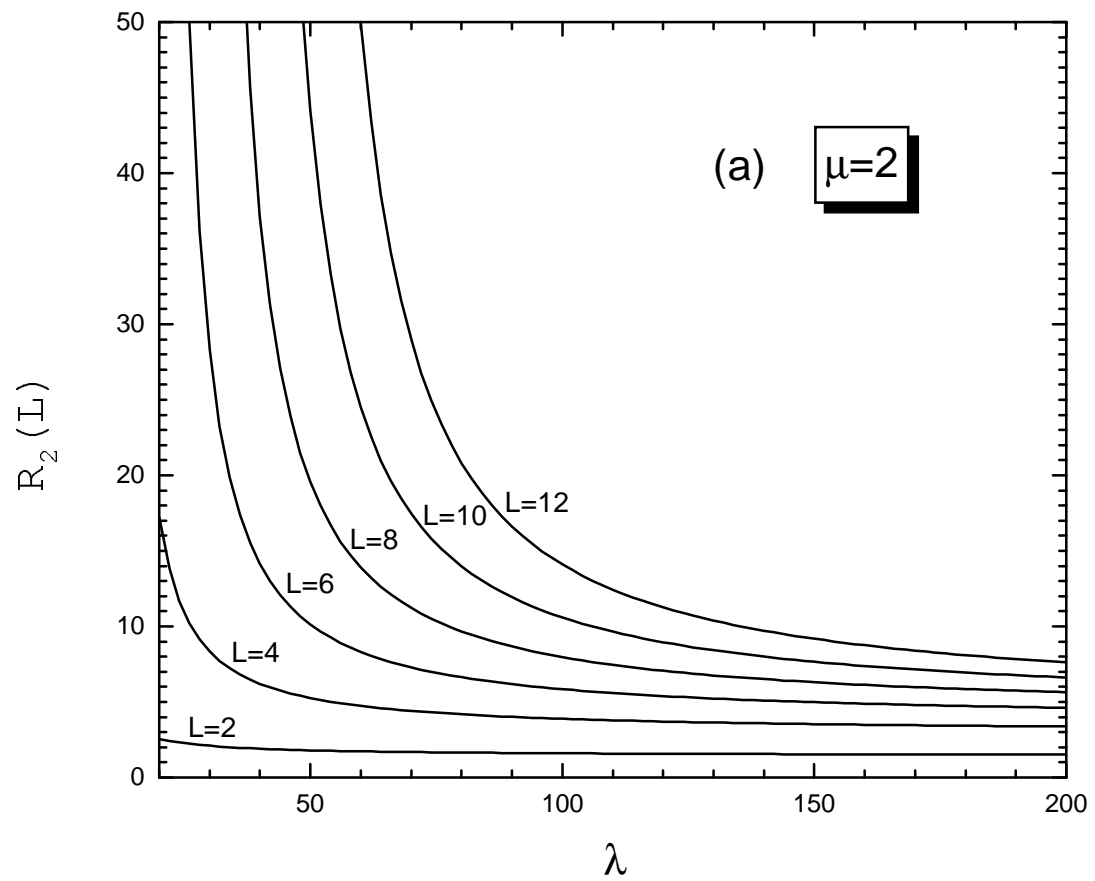


Figure 6(b)

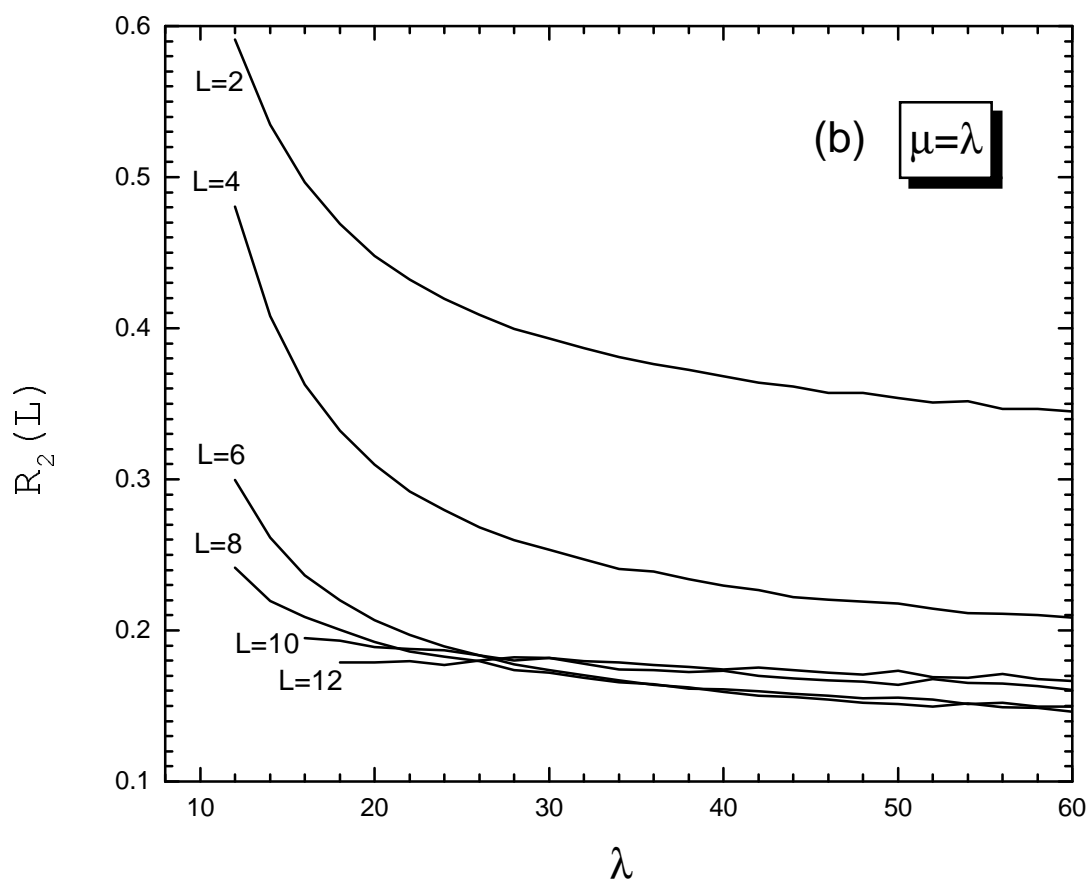


Figure 7 (a)

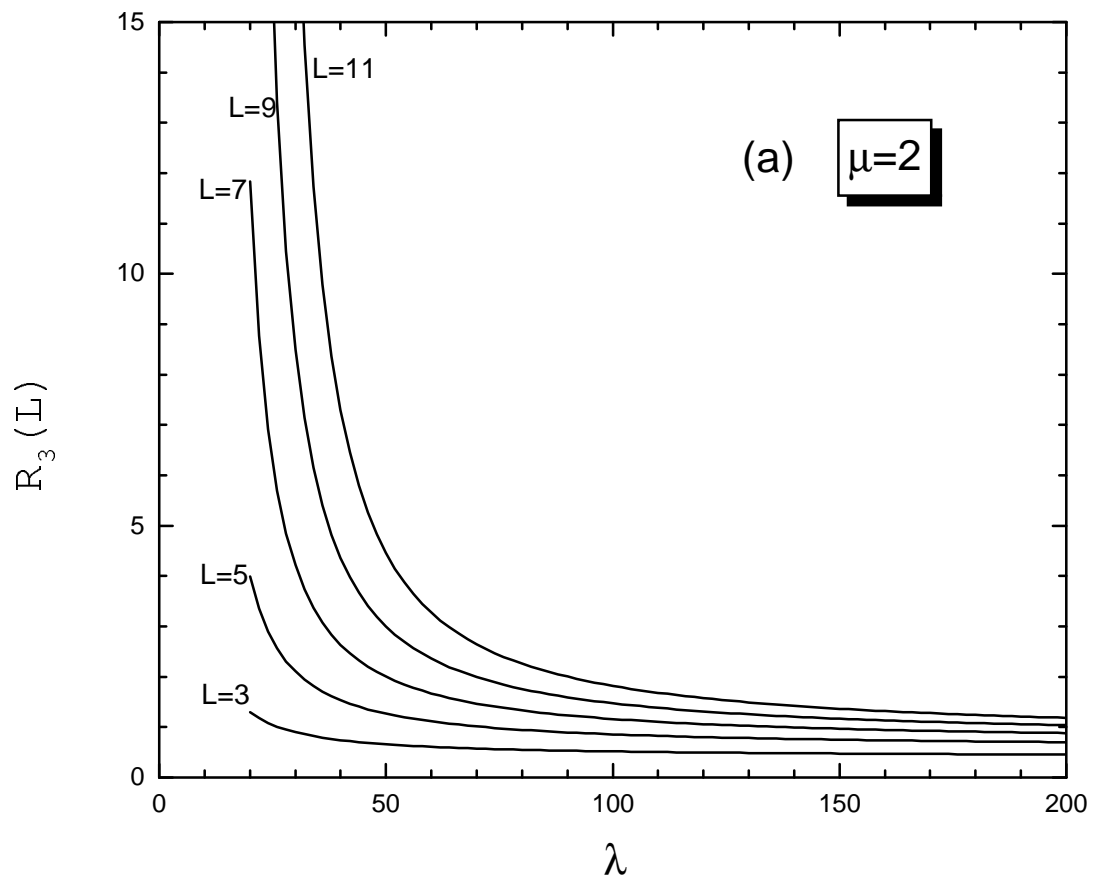


Figure 7(b)

